PHYSICAL REVIEW B **89**, 220503(R) (2014)

# Coexistence of orbital degeneracy lifting and superconductivity in iron-based superconductors

H. Miao,[1] L.-M. Wang,[2] P. Richard,[1,3,*] S.-F. Wu,[1] J. Ma,[1] T. Qian,[1] L.-Y. Xing,[1] X.-C. Wang,[1] C.-Q. Jin,[1,3] C.-P. Chou,[2,4] Z. Wang,[5] W. Ku,[2] and H. Ding[1,3,†]

[1]*Beijing National Laboratory for Condensed Matter Physics, and Institute of Physics, Chinese Academy of Sciences, Beijing 100190, China*
[2]*Condensed Matter Physics and Materials Science Department, Brookhaven National Laboratory, Upton, New York 11973, USA*
[3]*Collaborative Innovation Center of Quantum Matter, Beijing, China*
[4]*Beijing Computational Science Research Center, Beijing 100084, China*
[5]*Department of Physics, Boston College, Chestnut Hill, Massachusetts 02467, USA*

(Received 29 January 2014; revised manuscript received 29 May 2014; published 11 June 2014)

We report the angle-resolved photoemission spectroscopy observation of the lifting of symmetry-protected band degeneracy, and consequently the breakdown of local tetragonal symmetry in the superconducting state of Li($Fe_{1-x}Co_x$)As. Supported by theoretical simulations, we analyze the doping and temperature dependences of this band splitting and demonstrate an intimate connection between ferro-orbital correlations and superconductivity.

DOI: 10.1103/PhysRevB.89.220503 PACS number(s): 74.25.Jb, 74.20.Mn, 74.70.Xa, 79.60.−i

In contrast to conventional superconducting (SC) materials, superconductivity in high-temperature superconductors (HTSCs) usually emerges in the presence of other fluctuating orders with similar or higher-energy scales [1–4], thus instigating debates over their relevance for the SC pairing mechanism. Although spin fluctuations are widely believed to be crucial for unconventional superconductivity, orbital fluctuations in the multiorbital iron-based superconductors (IBSCs) are proposed to be directly responsible for the structural phase transition [5,6] and closely related to the observed giant magnetic anisotropy and electronic nematicity [7–13]. More recently, fluctuating orbital order has been proposed to lead to an attractive mechanism for pairing [14,15] and further raised the following question: Can superconductivity coexist with or even emerge from orbital fluctuations?

In the tetragonal phase without spin-orbital coupling (SOC), the $d_{xz}/d_{yz}$ orbitals are degenerate at the Brillouin zone center (Γ point), which is guaranteed by point-group symmetry. Ferro-orbital (FO) order, which leads to unequal occupation of the $d_{xz}/d_{yz}$ orbitals, would lift the degeneracy at Γ, resulting in a band gap $\Delta_{\text{band}}$ that can be monitored directly by angle-resolved photoemission spectroscopy (ARPES). While FO fluctuations have been proposed as the origin of electronic nematicity [5,6] and can be closely related to the emergence of superconductivity [14,15], probing FO fluctuations directly in the absence of structural and magnetic phase transitions needs to be explored, and whether FO fluctuations coexist or compete with the SC order is still an open question.

In this Rapid Communication, we report the ARPES observation of the lifting of symmetry-protected band degeneracy, and consequently the breakdown of local tetragonal symmetry in the SC state of Li($Fe_{1-x}Co_x$)As. By analyzing the doping and temperature dependences of this band splitting and using theoretical simulations, we demonstrate that the splitting is caused by power-law decayed ferro-orbital correlations and prove its intimate connection with superconductivity.

Single crystals of $LiFe_{1-x}Co_xAs$ were synthesized by a self-flux method using $Li_3As$, $Fe_{1-x}Co_xAs$, and As powders as the starting materials. The mixture was grounded and put into alumina crucible and sealed in Nb crucibles under 1 atm of argon gas. The Nb crucible was then sealed in an evacuated quartz tube, heated to 1100 °C, and slowly cooled down to 700 °C at a rate of 3 °C/h. High-energy resolution ARPES data were recorded at the Institute of Physics, Chinese Academy of Sciences, using the He Iα ($h\nu = 21.2$ eV) resonance line of an helium discharge lamp. The angular and momentum resolutions were set to 0.2° and 3 meV, respectively. ARPES polarization measurements were performed at beamlines PGM and Apple-PGM of the Synchrotron Radiation Center (Wisconsin) equipped with a Scienta R4000 analyzer and a Scienta SES 200 analyzer, respectively. The energy and angular resolutions were set at 20 meV and 0.2°, respectively. All samples were cleaved *in situ* and measured in a vacuum better than $3 \times 10^{-11}$ Torr.

In addition to having a natural nonpolar cleaving surface preserving its bulk properties [16–18], Li($Fe_{1-x}Co_x$)As has neither structural nor magnetic phase transitions in its whole phase diagram [19], enabling us to study fluctuations in the absence of long-range orders. In Fig. 1, we compare the electronic band dispersion of LiFeAs and $LiFe_{0.88}Co_{0.12}As$ at 20 K around the Γ point. Our polarization analysis confirms that the α and α′ bands, which are mainly composed of $d_{xz}/d_{yz}$ orbitals, have odd and even symmetries, respectively [20–22]. The extracted band dispersion [23] in $LiFe_{0.88}Co_{0.12}As$ ($T_c = 4$ K) indicates that both the α and α′ bands sink below $E_F$ and are exactly degenerate at the Γ point, as required by symmetry. In contrast, the α band crosses $E_F$ at $k_F = 0.03\pi/a$ in the parent compound LiFeAs ($T_c = 18$ K), whereas the top of the α band lies about 12 meV below $E_F$, which means that the $d_{xz}/d_{yz}$ orbitals are split in LiFeAs without long-range magnetic and orbital orders. To precisely resolve the band splitting, we recorded very-high-energy resolution ARPES intensity plots of LiFeAs and $LiFe_{0.88}Co_{0.12}As$, as shown in Fig. 1. From the high-resolution data, we evaluate the band gap to $\Delta_{\text{band}} \sim 14$ meV in LiFeAs by extrapolating the top of the α band using a parabolic fit, and we confirm the degeneracy of the $d_{xz}/d_{yz}$ bands in

*p.richard@iphy.ac.cn
†dingh@iphy.ac.cn

 

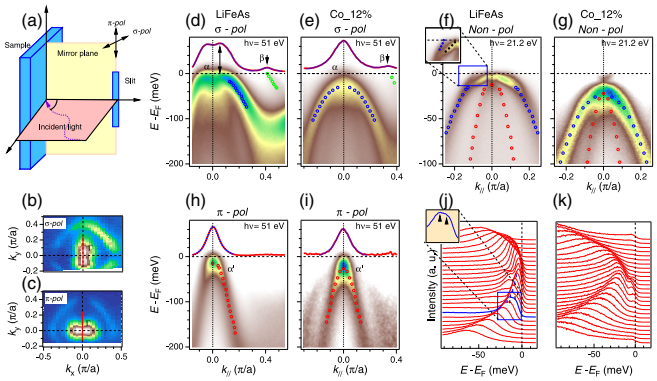


FIG. 1. (Color online) (a) ARPES experimental geometry. (b), (c) FS mapping at the Brillouin zone center measured under $\sigma$ and $\pi$ configurations. (d), (h) ARPES intensity plots of LiFeAs measured along the $\Gamma$-$M$ direction [the red line in (b) and (c)], and recorded with 51 eV incident light in the $\sigma$ and $\pi$ configurations to select odd and even orbital symmetries [20–22], respectively. (e), (i) Same as (d) and (h), but for $LiFe_{0.88}Co_{0.12}As$. (f), (g) High-energy resolution ARPES cuts along the $\Gamma$-$M$ direction of LiFeAs and $LiFe_{0.88}Co_{0.12}As$, respectively, recorded with the He I$\alpha$ line of an helium discharge lamp. The red and blue curves in (d), (e), (h), and (i) are the original and fitted momentum distribution curves at $E_F$, respectively. The blue, red, and green circles represent the peak positions associated with the $\alpha$ ($d_{\text{odd}}$), $\alpha'$ ($d_{\text{even}}$), and $\beta$ ($d_{xy}$) bands, respectively, where $d_{\text{odd}}$ ($d_{\text{even}}$) is the odd (even) linear combination of the $d_{xz}$ and $d_{yz}$ orbitals. (j), (k) EDCs corresponding to the data shown in (f) and (g), respectively. The blue EDC in (j), also shown in inset, illustrates the splitting of the $\alpha$ band.

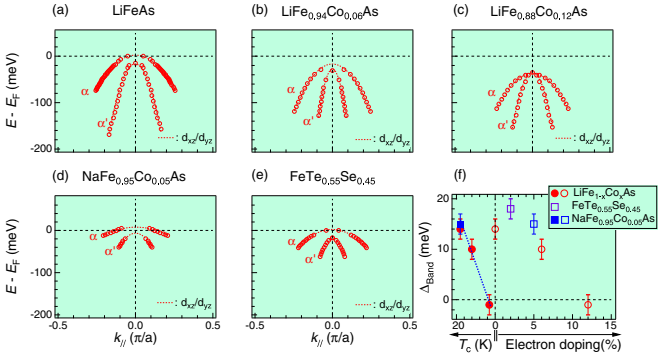


FIG. 2. (Color online) (a)–(c) Extracted band dispersion of the $d_{xz}/d_{yz}$ bands in LiFeAs, $LiFe_{0.94}Co_{0.06}As$ [22], and $LiFe_{0.88}Co_{0.12}As$, respectively. (d), (e) Extracted band dispersion of $NaFe_{0.95}Co_{0.05}As$ [26] and $FeTe_{0.55}Se_{0.45}$ [27], respectively. Red dashed curves are parabolic fits. (f) Doping and $T_c$ dependence of $\Delta_{\text{band}}$. The open and solid symbols refer to the doping (bottom right) and $T_c$ (bottom left) axes. Error bars are determined by standard deviation of the fitting parameters [22].

$LiFe_{0.88}Co_{0.12}As$. By zooming near $E_F$, we find that the $\alpha$ band further splits into two branches, as shown in Figs. 1(f) and 1(j). While one branch is the continuous extension of the high binding energy dispersion, the other one shows an inflection point at 14 meV binding energy. A similar effect is also observed on the electron band [22] and, as discussed later, the observed fine structure is caused by twin domains and supports that the observed band splitting is caused by FO fluctuations. As reported previously [24], we distinguish an electron band at the $\Gamma$ point of electron-doped $LiFe_{0.88}Co_{0.12}As$, which is not clear in the synchrotron-based results, most likely due to different $k_z$ positions. We suspect that this small electron band has a strong As $p_z$ orbital component and is similar to the one observed in $(Tl,Rb)_yFe_{2-x}Se_2$ [25].

To check whether the $d_{xz}/d_{yz}$ splitting is a general feature of the IBSCs, we performed similar experiments on various materials and summarized the results in Fig. 2. We first considered $LiFe_{0.94}Co_{0.06}As$ ($T_c = 10$ K), which has an intermediate doping between LiFeAs and $LiFe_{0.88}Co_{0.12}As$ [22]. Unlike in LiFeAs and similarly to $LiFe_{0.88}Co_{0.12}As$, the $\alpha$ band falls below $E_F$. For this material, we find $\Delta_{\text{band}} = 10$ meV, suggesting that the band splitting is gradually suppressed as $T_c$ decreases from 18 to 4 K. We also studied the band splitting in $NaFe_{0.95}Co_{0.05}As$ ($T_c = 18$ K) [26], which is isostructural to LiFeAs (the so-called 111 structure). From the extracted band dispersions displayed in Fig. 2(d), we deduce that $\Delta_{\text{band}} = 15$ meV in this particular compound. Interestingly, as shown in Fig. 2(f), all our data on the 111 crystal structure indicate that $\Delta_{\text{band}}$ scales with $T_c$ in this family of materials, suggesting that the band splitting might be related to superconductivity. Interestingly, there is at least one other IBSC for which a $d_{xz}/d_{yz}$ band splitting is clearly observed. Indeed, this observation has been reported for the $FeTe_{1-x}Se_x$ family of IBSCs [27,28]. Using the data from Miao *et al.* [27], reproduced in Fig. 2(e), we find that $\Delta_{\text{band}} = 18$ meV in $FeTe_{0.55}Se_{0.45}$, which is even larger than in LiFeAs. The observed band splitting in all the IBSCs studied here strongly suggests that the $d_{xz}/d_{yz}$ separation at the $\Gamma$ point has a fundamental origin.

We now focus on the temperature evolution of $\Delta_{\text{band}}$ in LiFeAs. For this purpose, we show in Fig. 3 high-energy resolution ARPES cuts across the $\Gamma$ point recorded between 50 and 250 K. The data are divided by the Fermi-Dirac function convoluted by the resolution function to reveal the band dispersion above $E_F$, which are obtained from parabolic fits. While the linewidths of the $\alpha'$ and $\beta$ bands broaden with temperature, their dispersions are unaffected. The $\alpha$ band, on the other hand, gradually shifts downward and its top almost merges with that of the $\alpha'$ band at 250 K. In Fig. 3(m), we show the evolution of $\Delta_{\text{band}}$ as a function of temperature by using different methods that all show that the $d_{xz}/d_{yz}$ splitting decreases gradually from nearly 0 at 250 K to about 14 meV at 50 K [22]. Interestingly, the splitting survives even below the SC phase transition at 18 K. As shown in Figs. 3(n)–3(p), the $\alpha$ band opens up a SC gap below $T_c$, whereas the $\alpha'$ band is barely changed. This observation proves that the band splitting coexists with superconductivity.

The observed degeneracy lifting by ARPES at the $\Gamma$ point reflects directly the difference in site energy of the $d_{xz}$ and $d_{yz}$ orbitals at low energies, which is a direct measurement of the ferro-orbital configuration, regardless of the origin of the mechanism driving the system into this configuration. In order to demonstrate that FO fluctuations can lead to the removal of a symmetry-imposed degeneracy, even in the absence of long-range ordering, we investigate a simple model of a quasi-one-dimensional (1D) electronic system (since $d_{xz}/d_{yz}$ orbitals have strongly anisotropic quasi-1D hopping integrals) under the influence of a spatially fluctuating local FO order parameter (represented by a diagonal Ising field) [21,22], and

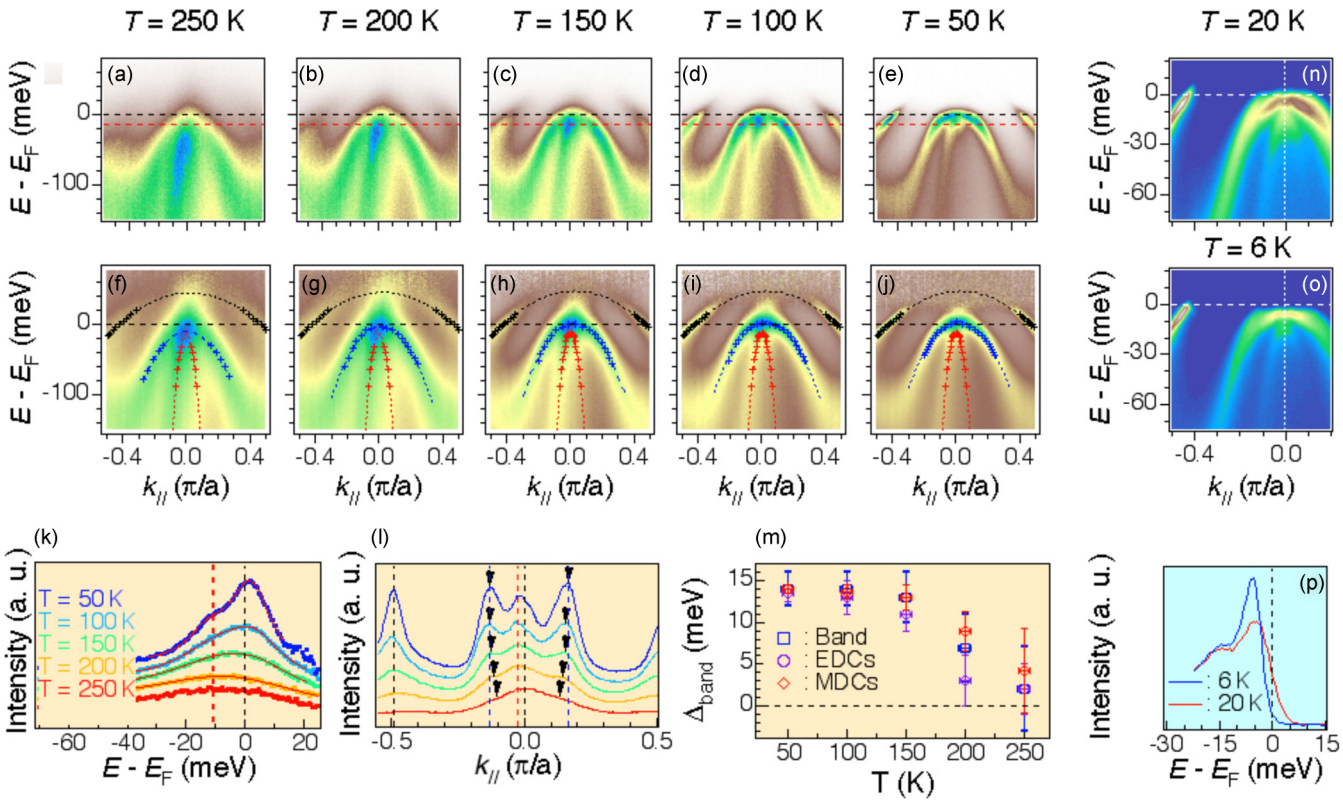


FIG. 3. (Color online) (a)–(e) High-energy resolution ARPES intensity plots at $T = 250$, 200, 150, 100, and 50 K, respectively. (f)–(j) Same data but divided by the Fermi-Dirac function convoluted with the system resolution function to probe the electronic structure above $E_F$. Band dispersions at different temperatures are extracted using momentum distribution curves (MDCs) and fitted to parabolic functions. (k) Energy distribution curves (EDCs) at the Γ point at different temperatures. We used two Lorentzian peaks to extract the top of the $\alpha$ and $\alpha'$ bands, and plot the fitted results on top of the original data using red dashed curves [22]. The top of the $\alpha$ band is shifted towards high binding energy as temperature increases, and it almost merges with the top of the $\alpha'$ band at 250 K. (l) MDCs recorded 20 meV below $E_F$, which corresponds to the red dashed lines shown in (a)–(e). At high temperature, the $\alpha$ peak positions move towards Γ, indicating that the band moves downward in energy. In contrast, the peak positions of the $\alpha'$ and $\beta$ bands are unchanged [22]. (m) Temperature evolution of $\Delta_{\text{band}}$. The values of $\Delta_{\text{band}}$ are extracted from the electronic band dispersions, EDCs and MDCs. Error bars are determined by the standard deviation of the fitted parameters. (n) and (o) are ARPES intensity plots just above and well below $T_c$, respectively. (p) EDCs at the Γ point above and below $T_c$.

we display the results in Fig. 4. When the local order parameter has only short-range correlations (exponential decay), no clear indication of the fluctuating order is observed in the electronic structure other than the scattering of the particle that broadens the spectral function, as illustrated in the top row of Fig. 4. In contrast, when the spatial correlations of the local order parameter are long ranged (power-law decay), the quasiparticle peak splits in two and a pseudogap in the spectral function develops in between, as shown in Figs. 4(f)–4(h). This pseudogap corresponds to the splitting of the degenerate bands shown in Fig. 1. Although the spectral function exhibits features identical to those expected in the presence of a macroscopic long-range order, we emphasize that the system has not yet developed a true order, but only long-range spatial correlations. In other words, the one-particle Green's function has gone ahead and reflects the underlying, almost ordered, electronic structure. Therefore, the experimentally observed doping-dependent splitting between the $d_{xz}/d_{yz}$ bands in the absence of FO order can be attributed to strong, slow-decaying, long-range FO correlations that cover a large region of the phase diagram and eventually support superconductivity at low temperature. We stress that although our minimal two-orbital model indicates that a fluctuating diagonal order parameter is capable of lifting a degeneracy required by symmetry, one should be cautious when comparing our models with realistic band structures. In real systems, the self-energy induced by the fluctuating ferro-orbital order parameter should be momentum, energy and orbital dependent, and thus exhibit rich variations.

Very recently, an electronic Raman scattering study of $Ba(Fe_{1-x}Co_x)_2As_2$ [29], an ARPES study [9], and a combined study of magnetic torque and x ray in $BaFe_2(As_{1-x}P_x)_2$ [13] reported electronic nematicity in the absence of a magnetic phase transition. The observed nematic signal persists far above the SC and structural phase transitions, indicating the presence of a strong fluctuating orbital order, which is consistent with our doping- and temperature-dependent results, as well as with our theoretical interpretation. However, alternative mechanisms could also lead indirectly to the lifting of the band degeneracy. For example, although the *C*-type (collinear) antiferromagnetic (AF) correlations do not directly contribute to the observed band degeneracy lifting, they could do so when coupled to the orbital degree of freedom, as predicted by theoretical studies [5,6,30,31]. Nevertheless, in the present study, we find that superconductivity emerges

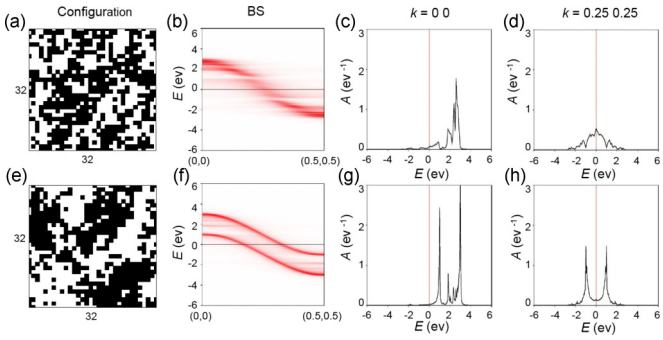


FIG. 4. (Color online) (a) An example of the configuration of a FO disordered system (represented by an Ising field) without long-range correlations. (b) The resulting average band structure that couples to the Ising field, showing no clear splitting of the band. (c), (d) The average spectral function at momentum $k = (0,0)$ and $k = (0.25,0.25)$. (e)–(h) Similar to (a)–(d), however, the disordered system contains long-range, power-law decaying correlations of the local order parameter.

in the regime of strong FO correlations and that the SC transition temperature scales with the strength of the local orbital order, suggesting an intimate connection between FO correlations and superconductivity. This observation is very important since a recent ARPES and NMR study reports enhancement of low-energy antiferromagnetic spin fluctuations in $LiFe_{1-x}Co_xAs$ samples with lower $T_c$ [24], thus suggesting that such low-energy antiferromagnetic fluctuations alone do not control the strength of superconductivity in $LiFe_{1-x}Co_xAs$.

Finally, we discuss the effect of SOC. In principle, SOC can lift the degeneracy of the $d_{xz}/d_{yz}$ orbitals at the $\Gamma$ point while maintaining global tetragonal symmetry [32]. However, since SOC is a local effect and barely changes with doping and temperature, our observation of $\Delta_{\text{band}}$ variations as a function of doping and temperature is inconsistent with this scenario. Moreover, we carefully extracted the electronic band structure near the $M$ point and found that the degeneracy between $d_{xz}$ and $d_{yz}$ at the $M$ point is lifted with a splitting gap $\Delta_M = 8$ meV, which is smaller than the splitting at the $\Gamma$ point [22]. All the experimental facts support our assumption that the observed $d_{xz}/d_{yz}$ splitting at the $\Gamma$ point is caused by FO fluctuations instead of SOC. Although spin fluctuations have been widely studied and discussed, few experimental studies on the orbital fluctuations can be found in the literature. Our study provides evidence for strong, long-range FO correlations in IBSCs and demonstrates their intimate connection with superconductivity in $LiFe_{1-x}Co_xAs$.

We thank A. Tsvelik, J.-P. Hu, F. Wang, P. D. Johnson, and H.-B. Yang for useful discussions. This work was supported by grants from CAS (No. 2010Y1JB6), MOST (No. 2010CB923000, No. 2011CBA001000, and No. 2013CB921703), and NSFC (No. 11004232 and No. 11274362). The theoretical study is supported by U.S. Department of Energy, Office of Science DE-AC02-98CH10886. This work is based in part on research conducted at the Synchrotron Radiation Center, which is primarily funded by the University of Wisconsin-Madison with the University of Wisconsin-Milwaukee.

[1] D. Aoki, A. Huxley, E. Ressouche, D. Braithwaite, J. Flouquet, J. Brison, E. Lhotel, and C. Paulsen, Nature (London) **413**, 613 (2001).
[2] J. M. Tranquada, H. Woo, T. G. Perring, H. Goka, G. D. Gu, G. Xu, M. Fujita, and K. Yamada, Nature (London) **429**, 534 (2004).
[3] J. M. Tranquada, J. D. Axe, N. Ichikawa, A. R. Moodenbaugh, Y. Nakamura, and S. Uchida, Phys. Rev. Lett. **78**, 338 (1997).
[4] D. K. Pratt, W. Tian, A. Kreyssig, J. L. Zarestky, S. Nandi, N. Ni, S. L. Bud'ko, P. C. Canfield, A. I. Goldman, and R. J. McQueeney, Phys. Rev. Lett. **103**, 087001 (2009).
[5] C.-C. Lee, W.-G. Yin, and W. Ku, Phys. Rev. Lett. **103**, 267001 (2009).
[6] W.-C. Lv, F. Krüger, and P. Phillips, Phys. Rev. B **82**, 045125 (2010).
[7] T.-M. Chuang, M. P. Allan, J. Lee, Y. Xie, N. Ni, S. L. Bud'ko, G. S. Boebinger, P. C. Canfield, and J. C. Davis, Science **327**, 181 (2010).
[8] J.-H. Chu, J. G. Analytis, K. D. Greve, P. L. McMahon, Z. Islam, Y. Yamamoto, and I. R. Fisher, Science **329**, 824 (2010).
[9] T. Shimojima *et al.*, Phys. Rev. B **89**, 045101 (2014).
[10] M. Yi, D.-H. Lu, J.-H. Chu, J. G. Analytis, A. P. Sorini, A. F. Kemper, B. Moritz, S. K. Mo, R. G. Moore, M. Hashimoto, W.-S. Lee, Z. Hussain, T. P. Devereaux, I. R. Fisher, and Z.-X. Shen, Proc. Natl. Acad. Sci. USA **108**, 6878 (2011).
[11] M. Yi, D. H. Lu, R. G. Moore, K. Kihou, C.-H. Lee, A. Iyo, H. Eisaki, T. Yoshida, A. Fujimori, and Z. X. Shen, New J. Phys. **14**, 073019 (2012).
[12] H.-H. Hung, C. L. Song, X. Chen, X. Ma, Q. K. Xue, and C. Wu, Phys. Rev. B **85**, 104510 (2012).
[13] S. Kasahara, H. J. Shi, K. Hashimato, S. Tonegawa, Y. Mizukami, T. Shibauchi, K. Sugimoto, T. Fukuda, T. Terashima, A. H. Nevidomskyy, and Y. Matsuda, Nature (London) **486**, 382 (2012).
[14] H. Kontani and S. Onari, Phys. Rev. Lett. **104**, 157001 (2010).
[15] S. Zhou, G. Kotliar, and Z. Wang, Phys. Rev. B **84**, 140505 (2011).
[16] K. Umezawa, Y. Li, H. Miao, K. Nakayama, Z.-H. Liu, P. Richard, T. Sato, J. B. He, D.-M. Wang, G. F. Chen, H. Ding, T. Takahashi, and S.-C. Wang, Phys. Rev. Lett. **108**, 037002 (2012).
[17] S. V. Borisenko, V. B. Zabolotnyy, D. V. Evtushinsky, T. K. Kim, I. V. Morozov, A. N. Yaresko, A. A. Kordyuk, G. Behr, A. Vasiliev, R. Follath, and B. Büchner, Phys. Rev. Lett. **105**, 067002 (2010).
[18] M. P. Allan, A. W. Rost, A. P. Mackenzie, Y. Xie, J. C. Davis, K. Kihou, C. H. Lee, A. Iyo, H. Eisaki, and T.-M. Chuang, Science **336**, 563 (2012).
[19] X.-C. Wang, Q. Q. Liu, Y. X. Lv, W. B. Gao, L. X. Yang, R. C. Yu, F. Y. Li, and C. Q. Jin, Solid State Commun. **148**, 538 (2008).

[20] X.-P. Wang, P. Richard, Y.-B. Huang, H. Miao, L. Cevey, N. Xu, Y.-J. Sun, T. Qian, Y.-M. Xu, M. Shi, J.-P. Hu, X. Dai, and H. Ding, Phys. Rev. B **85**, 214518 (2012).

[21] C.-H. Lin, T. Berlijn, L.-M. Wang, C.-C. Lee, W.-G. Yin, and W. Ku, Phys. Rev. Lett. **107**, 257001 (2011).

[22] See Supplemental Material at http://link.aps.org/supplemental/10.1103/PhysRevB.89.220503 for additional details of data analysis and theoretical support.

[23] P. D. Johnson, T. Valla, A. V. Fedorov, Z. Yusof, B. O. Wells, Q. Li, A. R. Moodenbaugh, G. D. Gu, N. Koshizuka, C. Kendziora, S. Jian, and D. G. Hinks, Phys. Rev. Lett. **87**, 177007 (2001).

[24] Z.-Y. Ye, M. Xu, Q. Q. Ge, Q. Fan, F. Chen, J. Jiang, P. S. Wang, J. Dai, W. Yu, B. P. Xie, and D. L. Feng, arXiv:1303.0682.

[25] Z.-H. Liu, P. Richard, N. Xu, G. Xu, Y. Li, X.-C. Fang, L.-L. Jia, G.-F. Chen, D.-M. Wang, J.-B. He, T. Qian, J.-P. Hu, H. Ding, and S.-C. Wang, Phys. Rev. Lett. **109**, 037003 (2012).

[26] Z.-H. Liu, P. Richard, K. Nakayama, G.-F. Chen, S. Dong, J.-B. He, D.-M. Wang, T.-L. Xia, K. Umezawa, T. Kawahara, S. Souma, T. Sato, T. Takahashi, T. Qian, Y.-B. Huang, N. Xu, Y.-B. Shi, H. Ding, and S.-C. Wang, Phys. Rev. B **84**, 064519 (2011).

[27] H. Miao, P. Richard, Y. Tanaka, K. Nakayama, T. Qian, K. Umezawa, T. Sato, Y.-M. Xu, Y.-B. Shi, N. Xu, X.-P. Wang, P. Zhang, H.-B. Huang, Z.-J. Xu, J. S. Wen, G.-D. Gu, X. Dai, J.-P. Hu, T. Takahashi, and H. Ding, Phys. Rev. B **85**, 094506 (2012).

[28] S.-Y. Tan, Y. Zhang, M. Xia, Z. R. Ye, F. Chen, X. Xie, R. Peng, D. F. Xu, Q. Fan, H. C. Xu, J. Jiang, T. Zhang, X. C. Lai, T. Xiang, J. P. Hu, B. P. Xie, and D. L. Feng, Nat. Mater. **12**, 634 (2013).

[29] Y. Gallais, R. M. Fernandes, I. Paul, L. Chauviere, Y. X. Yang, M.-A. Measson, M. Cazayous, A. Sacuto, D. Colson, and A. Forget, Phys. Rev. Lett. **111**, 267001 (2013).

[30] M. Daghofer, Q.-L. Luo, R. Yu, D. X. Yao, A. Moreo, and E. Dagotto, Phys. Rev. B **81**, 180514 (2010).

[31] R. M. Fernandes, A. V. Chubokov, J. Knolle, I. Eremin, and J. Schmalian, Phys. Rev. B **85**, 024534 (2012).

[32] V. Cvetkovic and O. Vafek, Phys. Rev. B **88**, 134510 (2013).